

Earthquake Stability Analysis of Rock Slopes: a Case Study

Shilpa Pal · Amir M. Kaynia · Rajinder K. Bhasin ·
D. K. Paul

Received: 14 December 2009 / Accepted: 23 March 2011 / Published online: 7 April 2011
© Springer-Verlag 2011

Abstract Stability analysis of Surabhi landslide in the Dehradun and Tehri districts of Uttaranchal located in Mussoorie, India, has been simulated numerically using the distinct element method focusing on the weak zones (fracture). This is an active landslide on the main road toward the town centre, which was triggered after rainfall in July–August 1998. Understanding the behaviour of this landslide will be helpful for planning and implementing mitigation measures. The first stage of the study includes the total area of the landslide. The area identified as the zone of detachment is considered the most vulnerable part of the landslide. Ingress of water and increased pore pressures result in reduced mobilized effective frictional resistance, causing the top layer of the zone of detachment to start moving. The corresponding total volume of rock mass that is potentially unstable is estimated to 11.58 million m³. The second stage of this study includes a 2D model focussing only on the zone of detachment. The

result of the analyses including both static and dynamic loading indicates that most of the total displacement observed in the slide model is due to the zone of detachment. The discontinuum modelling in the present study gives reasonable agreement with actual observations and has improved understanding of the stability of the slide slope.

Keywords UDEC · Earthquake · Rock slope · Discontinuities · Sliding · Rotation · Landslide

1 Introduction

Jointed rock mass response to load is governed by movements on pre-existing joints separating the blocks of intact rocks. Due to the fact that joints constitute the weakest zones of rock masses, the anisotropy created by the joints is of significance. In particular, in jointed rock slopes the joints give rise to the usual mechanisms of planar, wedge and toppling failure (Giani 1992; Goodman 1989; Hoek and Bray 1981; Hudson and Harrison 1997).

It is well known that the properties of a rock mass depend not only on the properties of the intact rock and the joints individually, but also how they interact. The stability of jointed rock masses may be strongly affected by the resistance of joints for which the most important characteristics are those associated with failure by slip. However, for high slopes or weak and closely jointed materials, failure is less constrained by individual joints; in such cases, rock mass failures involving general failure surfaces become more likely. This implies that the failure mechanism is not solely controlled by the joint pattern, and a failure surface can develop through intact rock. The majority of current design methods available for

S. Pal
School of Architecture and Built Environment,
Gautam Buddha University, Greater Noida, India
e-mail: shilpa@gbu.ac.in

A. M. Kaynia (✉)
Computational Geomechanics, NGI, PO Box 3930,
Ullevaal Stadion, 0806 Oslo, Norway
e-mail: Amir.M.Kaynia@ngi.no

R. K. Bhasin
Rock and Foundation Engineering, NGI,
PO Box 3930, Ullevaal Stadion, 0806 Oslo, Norway
e-mail: Rajinder.Kumar.Bhasin@ngi.no

D. K. Paul
Department of Earthquake Engineering,
IIT Roorkee, Roorkee 247667, Uttarakhand, India
e-mail: dpaulfeq@gmail.com

performing rock slope stability analysis may be categorized as limit equilibrium methods, for which the failure surface can be approximated satisfactorily by a series of straight-line segments. These methods have several inherent weaknesses because they involve assumptions concerning the interaction between the intact rock and the joints. Consequently, the calculations performed using limit equilibrium methods do not necessarily produce realistic results in terms of the observed mechanical behaviour.

Several researchers have attempted to use continuum (finite element) and discontinuum (distinct element) techniques to study the behaviour of rock slopes. Some continuum codes can consider the effect of static and pseudo-static earthquake loading by applying a seismic load to each finite element in the model. Such approaches are useful for analysis of underground structures, but are considered inadequate for the dynamic analysis of rock slopes. In the pseudo-static analysis approach, the ground deformations and/or inertial forces are imposed as static loads and the rock–structure interaction does not include dynamic or wave propagation effects. When the stability of the rock slope is controlled by movement of joint-bounded blocks, the use of discontinuum discrete-element codes which allow fully dynamic analyses are more appropriate than the continuum codes [Cundall (1987); Lorig et al. (1991)]. Eberhardt and Stead (1998) and Stead et al. (2006) provide an example of dynamic distinct-element analysis of a natural rock slope in Western Canada. Bhasin and Kaynia (2004) illustrated the application of the dynamic plane-strain distinct element code UDEC (Itasca, 2004) to a 700-m-high Norwegian rock slope to estimate the rock volumes associated with a potential catastrophic rock failure. Liu et al. (2004) used UDEC to simulate the dynamic response of a jointed rock slope subjected to effects of an explosion. These studies have successfully demonstrated the use of UDEC in the simulation of the dynamic response of jointed rock slopes.

Landslides are a frequent natural hazard in the seismically active North-West part of the Indian Himalayas. In this study, an attempt has been made to model the Surabhi Landslide (longitude 78°02'–78°04'E and latitude 30°28'–30°31'N) in the Dehradun and Tehri districts of Uttarakhand located in Mussoorie, India (see Fig. 1). This landslide is active on the Mussoorie–Kempty main road joining Kempty Falls and downtown Mussoorie. The landslide was triggered by heavy rainfall in July–August 1998, blocking the road for about 15 days. The crown of the landslide (30°29'N and 78°03'E) is located at an elevation of about 1,650 m between 6 and 7 distance marker stones from Mussoorie, on the Mussoorie–Kempty road. A major resort hotel is located 50 m uphill in the crown portion of the landslide. Mussoorie International School and Polo ground are situated further upslope. The study carried out by Gupta

and Ahmad (2007) to link landslide activity to rainfall intensity concluded that a continuous threat is posed by this landslide, requiring particular evaluation during the rainy season and remediation measures to limit future damage in the area. With this background, 2-D and 3-D numerical discontinuum modelling was performed as part of the present study to understand the failure mechanism of the landslide. Modelling has been carried out with the distinct element method (UDEC and 3DEC, Itasca 2003) which has the capability to model rock slope stability under earthquake loading. Understanding the behaviour of the Surabhi landslide will also be helpful for planning and implementing landslide mitigation measures.

2 Geological Description of the Area

The scarp of the active landslide is located at an elevation of 1,650 m. The landslide has a depth of about 100 m at the crest gradually increasing to about 300 m in the central body (Fig. 2). The dip of the slip surface is about 60–70° due N 10°E. The landslide involved the displacement of Quaternary material up to a depth of about 30 m. Four major joint sets trending NE–SW, NNE–SSW, NNW–SSE and ESE–WSW fragment the rock mass into small pieces of about 3–4 cm lengths. The slide starts from the resort hotel and passes through agricultural fields. Along a total track length of 3.5 km, the landslide has affected 38 families and about 5 ha of agricultural land (Gupta and Ahmad 2007).

The slide movement can be divided into three zones (Figs. 2 and 3):

1. zone of detachment (1,650–1,325 m above msl),
2. zone of transportation (1,325–1,100 m above msl)
3. zone of accumulation (1,100–800 m above msl).

Figure 3 shows the site and three zones of the slide. The major sliding plane is in the upper part of the slope where the rock mass is highly jointed.

3 Modelling with UDEC

The mechanical behaviour of a jointed rock mass is strongly affected by the behaviour of discontinuities which therefore plays an important role in the successful application of any numerical technique. The distinct element code (UDEC), incorporates the strength and deformability properties of the joints and intact rock and has been used for predicting the behaviour of Surabhi landslide. The analysis of rock slope stability is carried out in two parts. First the orientations of the major discontinuities that could result in the instability of the slope are analysed. Numerical

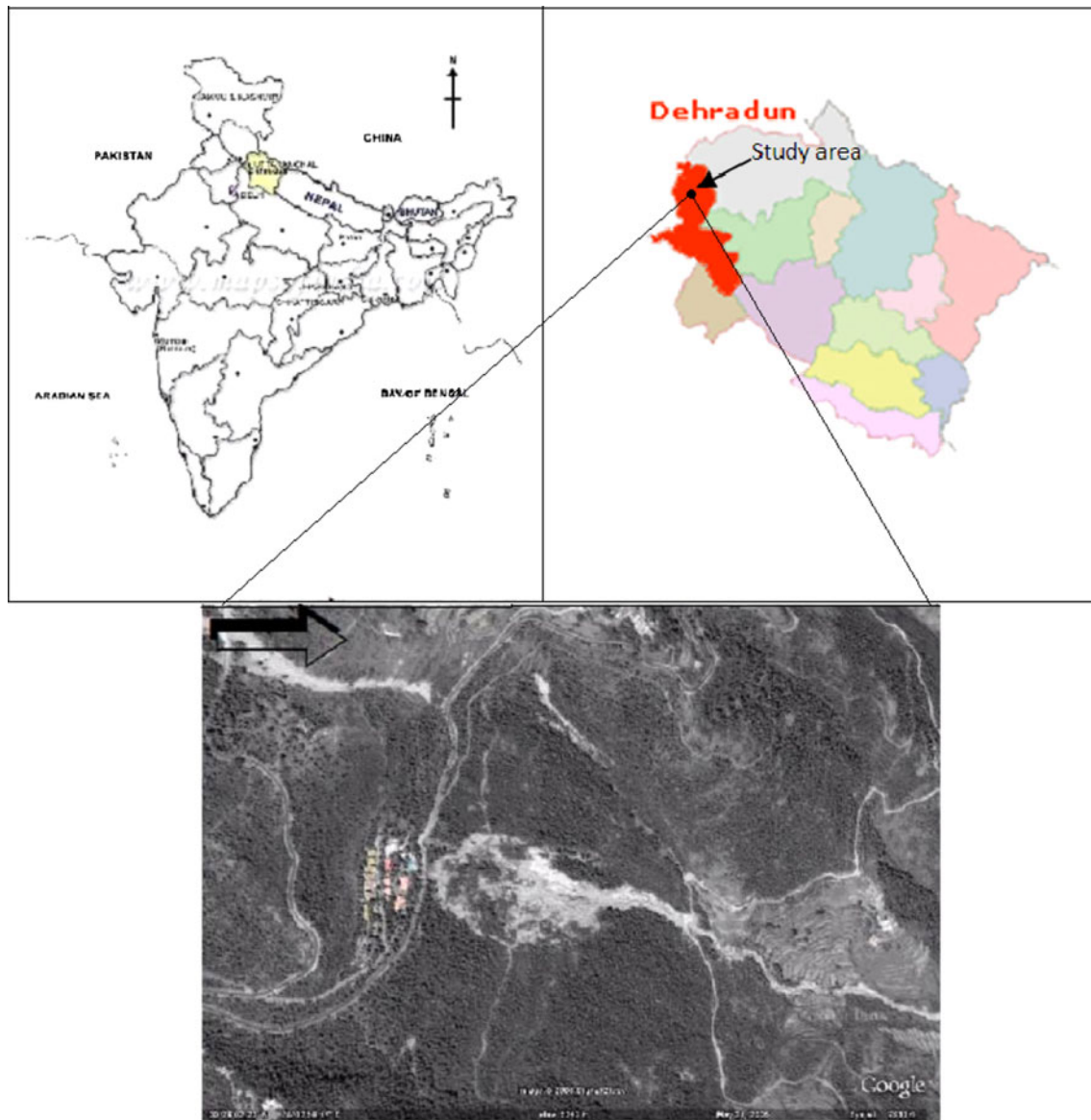


Fig. 1 Location map of study area

modelling is then performed under gravity load. According to geotechnical investigations carried out by Gupta and Ahmad (2007), it is clear that the rock in the zone of detachment is highly fractured and needs to be investigated with regard to stability.

Figure 4 shows the jointed slope model used in the 2-D numerical analysis. This simplified model was constructed based on the cross-section of the rock slope (Fig. 2) in Gupta and Ahmad (2007) and site visits during which the orientations of the joints were measured. Four joint sets are represented in the UDEC model. The purpose of numerical modelling in this case is to better understand the behaviour of the simplified rock slope model.

The overburden material on the top of the slide has not been considered, because the purpose of this study has been

to model the jointed slope without the unstable superficial loose material on the top. The number of joints represented in the model is reduced as compared to those present in the field and the relatively steep dipping foliations are probably up to five times longer than all but the persistent joints. The presence of long joints influences the displacements and deformation pattern of a rock slope when modelled using UDEC. If the rock block sizes are relatively large, then deformations will be mainly translational shear. However, if the block sizes are small, then rotation of rock blocks will also occur after some displacement due to translational shear.

Figure 4 shows the boundary conditions. Roller boundary conditions are assumed along the lateral sides of the model such that no displacement is allowed in the

Fig. 2 Cross-section of Surabhi Resort landslide (Gupta and Ahmad 2007). Figure shows the zone of detachment (1,650–1,325 m above the msl), zone of transportation (1,325–1,100 m above msl) and the zone of accumulation (1,100–800 m above msl)

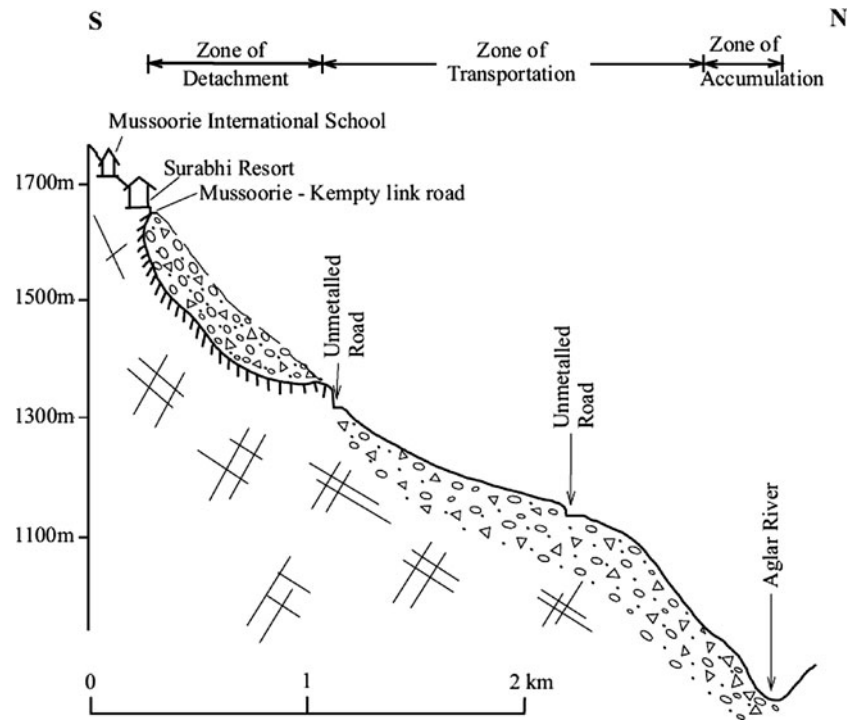


Fig. 3 Overview of Surabhi Resort Landslide. Black lines indicate the track length of 3.5 km

x-z-direction. At the base of the numerical model, the boundary is fixed such that no movement is allowed in either direction. The numbers in the model (Fig. 4) show the points under static conditions where displacement histories have been monitored.

3.1 Geotechnical Data of the Rock Mass

The rock mass around the landslide area has been classified using the RMR classification (Bieniawski 1979), the Q System (Barton et al. 1974) and the Geological Strength Index (GSI) (Hoek 1994). Based on a calculated RMR of 32, the rock mass is considered as poor quality (Gupta and

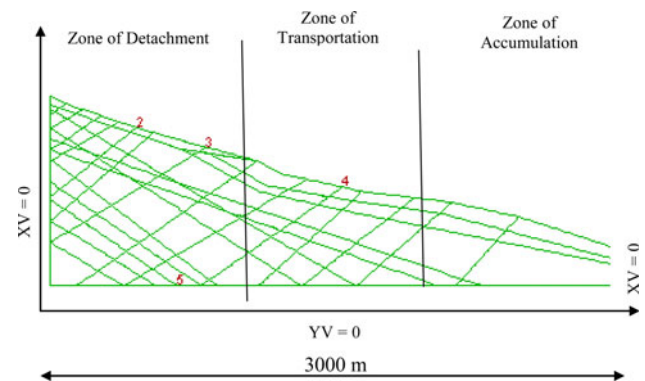
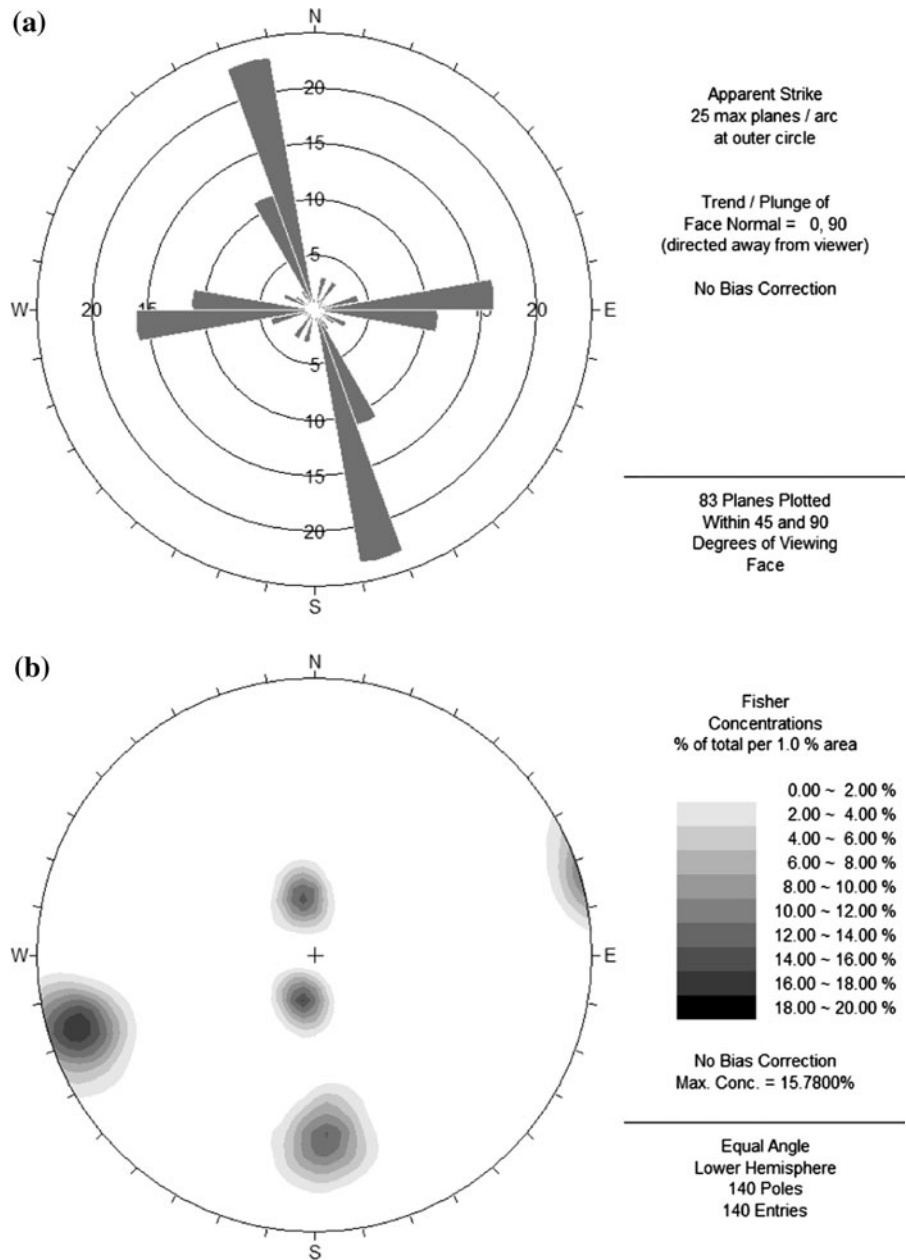


Fig. 4 Numerical model of the slope

Ahmad 2007). The conditions of the joints vary spatially; many have altered joint walls with mineral coatings, some have sandy-clay coatings, whereas others are tightly healed. Overall, the discontinuity condition can be described as damp with rock wall contact, often rough or irregular and stained. The average discontinuity spacing varies between 0.2 and 1 m. Many of the joints have a persistence of several meters, with some several tens of meters persistent.

Figure 5a and b shows, respectively a rose diagram of the joint orientations and a contour plot of the 4 joint sets described in Sect. 2 of the manuscript. Based on the relative weight of observational and laboratory-determined parameters, Gupta and Ahmad (2007) estimated a corresponding Q-value of the rock mass in the range 0.2–4, corresponding to a very poor to poor rock mass quality.

Fig. 5 Rose diagram of joint orientations and contour plot of joint sets



The uniaxial compressive strength of the intact rock was assumed to be 25 MPa and m_i of 8 for the limestone (Hoek 2000). Using Roclab (2007), GSI values yielded non-linear Hoek and Brown (1997) failure envelope and equivalent Mohr–Coulomb failure envelope. For the present landslide site, the equivalent cohesion and friction angle were found to be 0.18 MPa and 33°, respectively, again indicating a poor-quality rock mass for the purpose of slope stability. The intact rock is considered to behave as a linear-elastic material, whereas the rock discontinuities are assumed to behave as a linear-elastic perfectly plastic material. Table 1 shows the properties of the rock mass and joints used for the analysis.

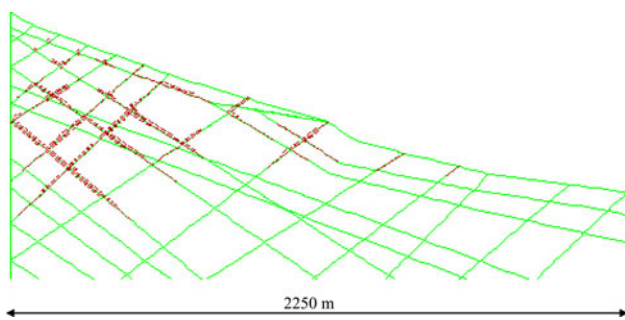
3.2 Static Analysis

Various cases were undertaken to study the stability of the Surabhi Landslide. Case 1 considered the initial static loading conditions. In this case the model was calibrated to represent the in situ conditions at the site. At the bottom of the slope, the vertical (total) stress was estimated at 28.78 MPa (density = 2,670 kg/m³, depth = 1,100 m). After simulating the in situ conditions, the gravity load was applied and the slope was monitored under static conditions until equilibrium was reached.

After gravity loading, it was observed that shearing of the joints took place in the zone of detachment, with

Table 1 Intact rock and joint parameters assumed for the UDEC analysis

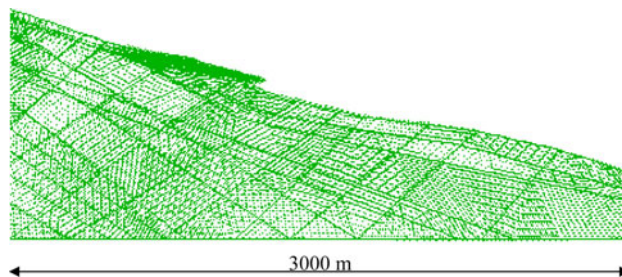
Rock type	Dolomitic limestone
Density	2,670 kg/m ³
Elastic modulus	20 GPa
Poisson's ratio	0.30
Bulk modulus	16.67 GPa
Shear modulus	7.692 GPa
Joint cohesion	0
Joint friction	33°
Joint normal stiffness	133 GPa/m
Joint shear stiffness	13.3 GPa/m
Joint tensile strength	0

**Fig. 6** Shearing of joints after gravity load in Case 1**Table 2** Displacement under static conditions for the three case studies

Cases		Static displacement	
		Shear disp. (mm)	Max. horizontal disp. (cm)
1	$JK_s = 13.3 \text{ GPa/m}$ $\phi = 33^\circ$	58	67
2	$JK_s = 13.3 \text{ GPa/m}$ $\phi = 30^\circ$	59	69
3	$JK_s = 13.3 \text{ GPa/m}$ $\phi = 22^\circ$	90	126

JK_s joint shear stiffness

maximum shear displacements along the joints of 58 mm and maximum net horizontal displacements of 67 cm. In the zone of transportation and accumulation, the slope is observed to be stable under the gravity load. Figure 6 shows the shearing along the joints. This figure clearly differentiates between shearing along the joints and the maximum net horizontal displacement. To further study the stability of the slope under saturated and weathering conditions, additional studies were performed.

**Fig. 7** Displacement under seismic excitation (sinusoidal wave)

3.2.1 Weathered Joint Conditions to Simulate Degradation of Joints

The study area is characterised by a sub-humid to humid temperate climate with winter precipitation. The average annual rainfall in the area varies between 2,000 and 3,000 mm with approximately three quarters of the rainfall falling during the monsoon season between July and September. Such an intensity of rainfall in a limited period contributes to weathering and degradation of the existing joints. Analysis of rainfall data during 1995–2005 indicates that area received about 2,376 mm of rainfall in a year out of which about 75% fell during July, August and September. During 1998, the area received an extraordinary rainfall of 5,117 mm, which is 2.2 times greater than the mean rainfall (Gupta and Ahmad 2007). It is this high-intensity of rainfall that triggered the landslide. As a result, in Case 2 it is assumed that there will be increased weathering of the joints due to ingress of water and climatic changes. This weathering leads to a reduction in shear strength along the joints, since the friction angle for unweathered dry rock surfaces is generally higher than for saturated and weathered surfaces. This effect has been simulated in the analysis by reducing the friction angle from 33° to 30° (Case 2). Such a reduction has previously been observed in laboratory residual tilt tests on saturated joint surfaces (e.g., Coulson 1972; Barton and Choubey 1977). Increased pore pressures in the joints will decrease the normal stress across the joints; however, because in situ joint apertures were not evaluated the pore pressures have not been considered directly in this model. Such effects may be evaluated using fully coupled groundwater mechanical analyses; however, the current study only used a corresponding reduction in friction angle. The reduction in friction angle causes an increase in the maximum horizontal displacement from 67 to 69 cm. Nonetheless, the slope remained stable with shear displacements only evident in the zone of detachment.

In Case 3, further parametric studies were performed by reducing the friction angle incrementally to 28°, 25° and 22°. These reductions are based on the mineralogical properties of the materials found in the discontinuities. For

example, joints with sandy-clay coatings may have friction angles in the range 20°–25° (Barton et al. 1974), whereas unaltered joint walls with surface staining may have friction angles between 30° and 35°. Although these reductions are crude estimates, the reduced friction angle of 22° causes a significant increase in the shear displacement of the joints, resulting in block movements. Table 2 summarises the displacements observed with the reduced friction angles.

3.3 Application of Dynamic Loading: Earthquake Conditions

Under earthquake loading, a base excitation is applied to the rock slope. It is important to analyse the slope for the actual seismic environment. The slope lies in zone IV as per the Criteria for Earthquake Resistant Design of Structures Part1: General Provisions and Buildings (IS Code 1893–2002). According to IS (1893) the area is highly seismic; this is confirmed by the number of earthquakes observed in the area in recent times. The analysis in this case starts from the end of Case 1 with the calculated stresses under gravity loading. Viscous boundary conditions are imposed to absorb the waves reaching the boundaries, thereby avoiding reflection of waves back into the model. The predominant frequency range depends on the medium and source of propagation. Measurement of the frequency at the rock site indicates that dominant frequencies are typically in the range 2–5 Hz. To account for this, the seismic analysis of the slope under study has been carried out using both real earthquake records and a sinusoidal wave of frequency 3 Hz for a period of 3 s applied as a shear wave at the base of the model. For the present analysis, the maximum ground velocity at the base of the model was taken as 0.162 m/s. This was calculated to correspond to the peak ground acceleration as observed in the Uttarkashi earthquake record of 20 October 1991. This occurred about 60 km from the city of Dehradun.

The excitation applied at the base of the model as a sinusoidal shear stress is calculated as follows:

$$\tau = V_s \rho v_{\max} \tag{1}$$

where ρ is the mass density of the rock and V_s is the shear wave velocity given by the following relationship:

$$V_s = \sqrt{\frac{G}{\rho}} = 1,700 \text{ m/s} \tag{2}$$

and G is the static shear modulus of the rock.

The above equation assumes isotropic conditions for simplicity. In order to compensate for the viscous boundary conditions, the shear stress applied at the base of the model as obtained by Eq. 1 was multiplied by a factor of 2 (Itasca 2004, UDEC version 4.0).

After the application of the 3 s sinusoidal excitation, it was observed that shearing became concentrated at the top of the slope in the zone of detachment. Shearing displacement increased from 58 mm to about 73 cm. The maximum horizontal displacement increased from 67 to 86 cm at the end of loading. Figure 7 shows the horizontal displacement, mainly in the top layer of the slope. A quiet period of 3 s was then simulated with an increase in displacement from 86 to 102 cm at the end of 6 s.

The acceleration time history of a realistic earthquake excitation has the appearance of a random signature of many cycles containing a wide spectrum of frequencies. The selected time histories should be representative of the seismicity of the region. This is usually defined in terms of a design response spectrum. For the present study, two time histories have been used. In this case, an acceleration time history compatible with the response spectrum of the site near the study area has been generated with peak ground acceleration (PGA) of 0.30 g and frequency range equivalent to the Uttarkashi earthquake record of 20 October 1991. The time history has been generated using the software WAVEGEN (Mukherjee and Gupta 2002). The transverse record of the generated time history has a PGA of 0.31 g and the vertical record has a PGA of 0.21 g. The predominant frequency content of the generated time history is 2.85 Hz. The generated time history is applied at the base of the model as a stress wave. The acceleration time history is first converted to a velocity time history, and then converted to a stress wave using the following equations (Itasca, 2004):

$$\tau_s = V_s \rho v_s \tag{3}$$

$$\tau_n = V_p \rho v_n \tag{4}$$

where v_s is the transverse velocity, v_n is the normal velocity, V_s is the shear wave velocity and V_p is the P-wave velocity calculated using Eq. 5

$$V_p = \sqrt{\frac{K + \frac{4G}{3}}{\rho}} \tag{5}$$

where K is the static bulk modulus.

The stress wave calculated using the above equations is applied at the base of the model with viscous boundary conditions at the base and on the sides. The applied record is 65 s long. The time step used by UDEC is $\Delta t = 1.232e-05$ s. As the wave propagates through the rock mass, amplification of the record is observed, as shown in Fig. 8. The plots of the computed velocity time histories at the face of the slope are displayed in Fig. 8.

The displacement observed after the application of the earthquake time history is 105 cm with a shear displacement of 10 cm. Shearing in this case is observed in the

Fig. 8 Time histories computed at the face of slope

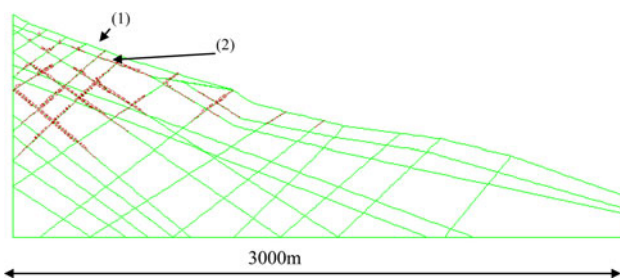
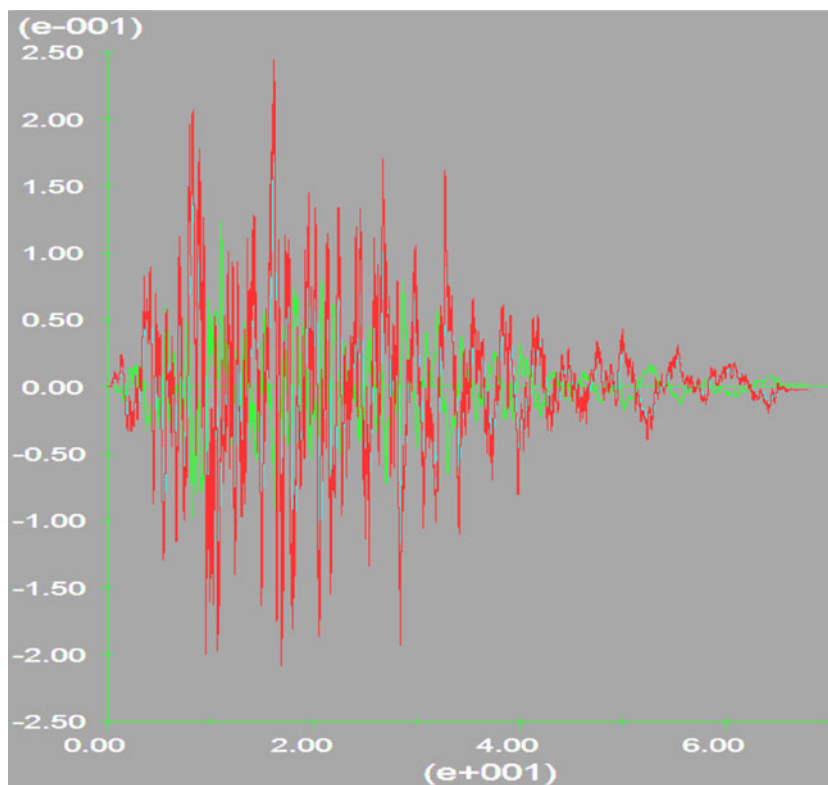


Fig. 9 Shearing of joints under seismic loading

zone of detachment. To have a better insight into the seismic analysis of the slope, another time history was synthetically generated to be compatible with the design response spectrum according to IS Code 1893-2002. The site is located in zone IV and the zone factor for this region is 0.24. Therefore, the artificial time history had a PGA 0.24 g in the transverse direction and 0.16 g in the vertical direction.

After application of the earthquake excitation, it was observed that the pattern of shear displacement is the same as was observed in the previous time history study. Figure 9 shows the observed shear displacement of the joints which in the order of 6.4 cm. The total displacement observed is 72 cm compared with 105 cm in the model with the real earthquake time history input and 102 cm with the sinusoidal wave excitation. Amplification of the input record was also observed. This comparison was made

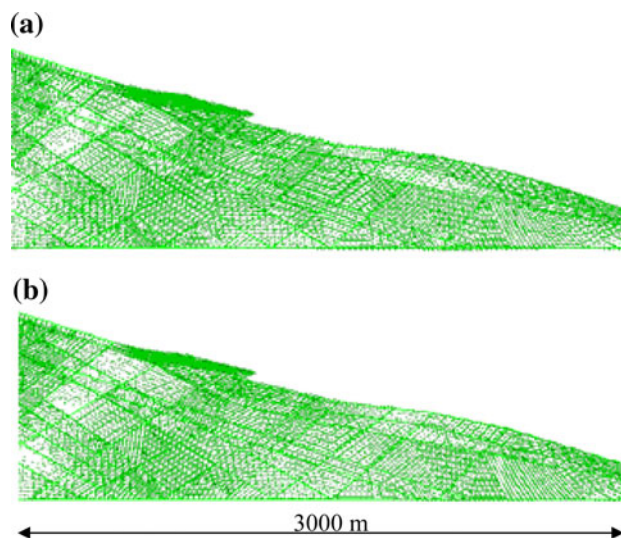
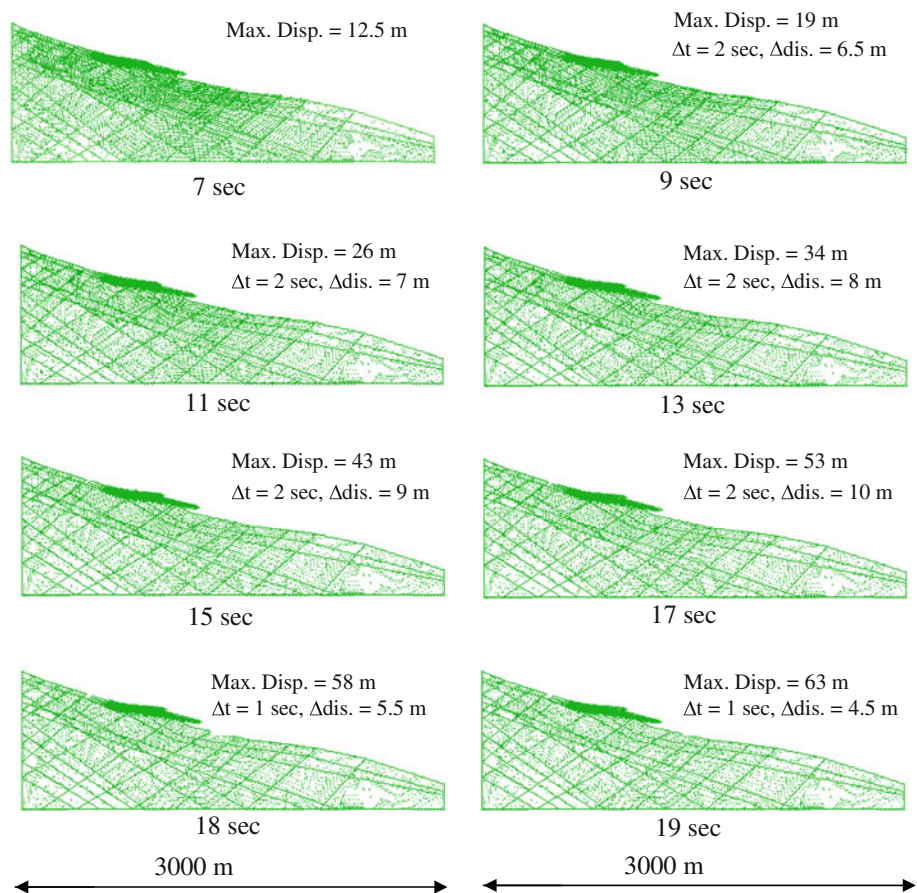


Fig. 10 Displacement of joints with Φ_r 30° under sinusoidal wave—**a** after 3 s, **b** after 6 s

by studying the response spectra recorded at points 1 and 2 marked on Fig. 9. These spectra clearly indicate that amplification of accelerations at point 1 is due to slipping of the shallow rock mass. This slipping has a particularly large effect on the high-frequency components of the input. As expected, the amplification is much higher at the slipping surface (i.e. uppermost layers where the blocks have started moving) than below the slipping plane.

Fig. 11 Failure mechanism for $\phi_r = 22^\circ$



Based on a comparison of the results obtained assuming different seismic environments, it can be concluded that under seismic conditions with the present rock mass and joint strength conditions, shearing of joints is predominant in the zone of detachment. To study the overall behaviour of the slope under seismic conditions, cases with reduced joint strength properties were studied. For these parametric analyses, only the sinusoidal wave model is used as seismic input. The results assuming a joint friction angle of 30° are shown in Fig. 10 and indicate that the horizontal displacement after 3 s is 90 cm (Fig. 10a) increasing to 110 cm after 6 s (Fig. 10b).

In the case with a reduced joint friction angle of 22° , horizontal displacement is observed in the top layers, which indicates that the reduced friction causes instability in both the zone of detachment and zone of transportation. This has major implications for the overall stability of the slope. The horizontal displacement after 3 s of the seismic input is 327 cm and increases to 981 cm after 6 s.

From the above cases of reduced friction angle under seismic input, it is clear that the slope is unstable in the zone of detachment along the top foliation plane. In the case with a reduced joint friction angle of 22° , the entire slope is unstable. This indicates that ingress of water and

the corresponding reduction of friction angle can be a significant hazard to the overall stability of the slope. To enhance understanding of the situation, the response of the slope was studied after the seismic excitation had ceased. Block failure of the top layer reaches a maximum down-slope horizontal displacement of 68 m. The failure mechanism is given in Fig. 11. The total volume of the rock mass that becomes unstable is 11.58 million m^3 .

The results given above show that degradation of the discontinuities due to water ingress can result in slope instability. Although pore water pressure is a major factor to the instability of the slope, this has not been simulated directly in this paper. Mitigation measures in this area include the provision of drainage holes spaced horizontally to allow drainage of excess water in the rock joints. Because the rock has a very low unconfined compressive strength (UCS), other stability measures such as bolting and shotcrete are likely to have limited impact.

4 UDEC Model: Zone of Detachment

From the preceding study it is clear that the zone of detachment is the most vulnerable part of the slope. To

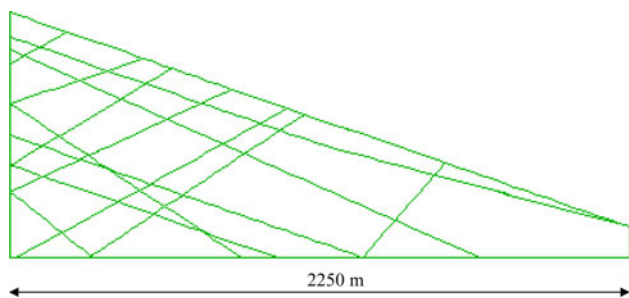


Fig. 12 Model of zone of detachment in UDEC

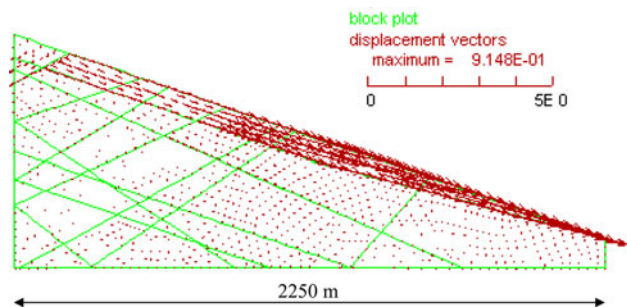


Fig. 13 Displacement at end of dynamic loading

investigate this in more detail, the zone of detachment alone was modelled in UDEC. The extent of the area used for studying the 2-D effect of the slide was 1,200 m in the x -direction and 500 m in the y -direction. The block material, joint properties and boundary conditions were similar to those assumed in the previous models. Figure 12 shows the model of the zone of detachment in UDEC.

Zoning of the blocks was undertaken to consider block deformability. First, the analysis was carried out with initial stresses and gravity load, until equilibrium was reached. It was observed that the slope is stable under gravity loading. The maximum horizontal displacement is 13 cm and joint shear displacement in the horizontal direction is 59 mm. The shear displacement is comparable with that observed in the full model but the total displacement is less. Shearing of the joints takes place at the end of the zone of detachment which is the same as observed for Case 1 previously.

After the static analysis, a dynamic analysis was carried out using a sinusoidal wave of frequency 3 Hz for 3 s. Boundary conditions were assumed viscous to absorb the outgoing waves. Shear displacements were observed to be concentrated in the upper foliation planes of the slope, which constitutes a highly weathered material in the field. The maximum horizontal displacement reaches 92 cm (Fig. 13) at the end of the seismic loading compared to a value of 86 cm observed in the full slope model. Table 3 shows a comparison of displacements for the zone of detachment for the static and dynamic analyses.

Table 3 Comparison of displacements for static and dynamic analysis

Cases	Static displacement		Dynamic displacement	
	Max.	Shear	Max.	Shear
Zone of detachment	13 cm	58 mm	92 cm	90 cm

From the modelling of the zone of detachment in UDEC, it is clear the total displacements observed in the full slope model, i.e. static and dynamic loading cases are in accordance with those observed in the present case. This observation therefore confirms that it is the zone of detachment which initiates the displacement in the Surabhi slide.

5 Conclusions

Numerical studies have been carried out in 2-D to predict the behaviour of the jointed rock slope in the Surabhi Resort landslide in Mussoorie, Garhwal Himalayas, India. Various cases have been simulated in order to improve understanding of the effect of static and dynamic loading, and to investigate the physics of the problem. Reduction of the friction angles in the joints causes a significant increase in shear displacements. The study concluded that the zone of detachment is the most vulnerable part of the slide. The analyses revealed that when the friction angle was reduced to account for ingress of water, the top layer of the zone of detachment started moving. This top layer in the field is the weathered material. The total volume of the rock mass that is potentially unstable is 11.58 million m^3 .

Analyses of static and dynamic loading indicate that most of the total displacement observed in the model occurs in the zone of detachment. The numerical results demonstrate that large dynamic motions result in instability of the upper layer of the slide. Both sliding and rotational displacements contribute to failure of the blocks.

Acknowledgments The authors gratefully acknowledge the anonymous reviewers for the constructive comments and suggestions which have significantly improved the quality of the paper. The cooperation and data provided by Dr. Vikram Gupta, Wadia Institute of Himalayan Geology, Dehradun, is highly appreciated. The authors would also like to gratefully acknowledge the financial support provided by the Norwegian Government through the Norwegian Royal Embassy in India.

References

- Barton N, Choubey V (1977) The shear strength of rock joints in theory and practice. *Rock Mech* 1–2:1–54
- Barton NR, Lien R, Lumsden A (1974) Engineering classification of rock masses for the design of tunnel support. *Rock Mech* 6:189–239

- Bhasin R, Kaynia AM (2004) Static and dynamic simulation of a 700 m high rock slope in western Norway. *Eng Geol* 71:213–260
- Bieniawski ZT (1979) The geomechanics classification in rock engineering applications. *Proceedings—4th international congress on rock mechanics*, ISRM, Montreaux, vol 2, pp 41–48
- Coulson JH (1972) Shear strength of flat surfaces in rock. In: *Proceedings—13th symposium on rock mechanics*, Urbana, III, American Society of Civil Engineers, NY, pp 77–105
- Cundall PA (1987) Distinct element models of rock and spoil structure. *Analytical and computational methods in engineering rock mechanics*, George Allen and Unwin, London, pp 129–136
- Eberhardt UE, Stead D (1998) Mechanisms of slope instability in thinly bedded surface mine slopes. In: Moore DP, Hungr O (eds) *Proceedings of 8th congress of the international association for engineering geology and environment*, Vancouver. Balkema, Rotterdam, pp 3011–3018
- Giani GP (1992) *Rock slope stability analysis*. A.A. Balkema, Rotterdam
- Goodman RE (1989) *Introduction to rock mechanics*, 2nd edn. Wiley and Sons, New York
- Gupta VK, Ahmad I (2007) Geotechnical estimation of Surabhi Resort Landslide in Mussoorie, Garhwal Himalayas, India. *Himal Geol* 28(2):21–32
- Hoek E (1994) Strength of rock and rock masses. *ISRM News J* 2(2):4–16
- Hoek E (2000) *Practical rock engineering*. Balkema, Netherlands, p 313
- Hoek E, Bray JW (1981) *Rock slope engineering*. Institute of Mining and Metallurgy, London
- Hoek E, Brown ET (1997) Practical estimation of rock mass strength. *Int J Rock Mech Min Sci Geomech Abstr* 34:1165–1186
- Hudson JA, Harrison JP (1997) *Engineering rock mechanics. An introduction to the principle*. Pergamon, Oxford
- IS 1893 (Part I) (2002) *Indian standard criteria for earthquake resistant design of Structures (5th revision)*, Bureau of Indian Standards, New Delhi
- Itasca (2003) *User guide manuals 3DEC version 3.0*
- Itasca (2004) *Dynamic analysis. User's guide UDEC version 4.0*
- Liu YQ, Li HB, Zhao J, Li JR, Zhou QC (2004) UDEC simulation for dynamic response of a rock slope subject to explosions. *Int J Rock Mech Min Sci* 41(3):474
- Lorig LJ, Hart RD, Cundall PA (1991) Slope stability analysis of jointed rock using the distinct element method. *Transportation Research Record* 1330, TRB, National Research Council, Washington, DC, pp 1–9
- Mukherjee S, Gupta VK (2002) Wavelet-based generation of spectrum-compatible time-histories. *Soil Dyn Earthq Eng* 22(9):799–804
- Roclab (2007) *Rocscience Geomechanics Software and Research*, Toronto, Canada (online) <http://download.rocscience.com/ordering/FreeDownloadsForm.asp>
- Stead D, Eberhardt UE, Coggan JS (2006) Developments in the characterisation of complex rock slope deformation and failure using numerical modelling techniques. *Eng Geol* 83:217–235